Amino-termini isoforms of the Slack K^+ channel, regulated by alternative promoters, differentially modulate rhythmic firing and adaptation

Maile R. Brown[1], Jack Kronengold[1], Valeswara-Rao Gazula[1], Charalampos G. Spilianakis[2], Richard A. Flavell[2], Christian A. A. von Hehn[1], Arin Bhattacharjee[4] and Leonard K. Kaczmarek[1,3]

[1]*Departments of Pharmacology,* [2]*Immunobiology,* [3]*Cellular and Molecular Physiology, Yale University School of Medicine, New Haven, CT 06520, USA*
[4]*Department of Pharmacology and Toxicology, SUNY Buffalo, Buffalo, NY 14214, USA*

The rates of activation and unitary properties of Na^+-activated K^+ (K_{Na}) currents have been found to vary substantially in different types of neurones. One class of K_{Na} channels is encoded by the *Slack* gene. We have now determined that alternative RNA splicing gives rise to at least five different transcripts for *Slack,* which produce Slack channels that differ in their predicted cytoplasmic amino-termini and in their kinetic properties. Two of these, termed Slack-A channels, contain an amino-terminus domain closely resembling that of another class of K_{Na} channels encoded by the *Slick* gene. Neuronal expression of *Slack-A* channels and of the previously described *Slack* isoform, now called *Slack-B*, are driven by independent promoters. *Slack-A* mRNAs were enriched in the brainstem and olfactory bulb and detected at significant levels in four different brain regions. When expressed in CHO cells, Slack-A channels activate rapidly upon depolarization and, in single channel recordings in *Xenopus* oocytes, are characterized by multiple subconductance states with only brief transient openings to the fully open state. In contrast, Slack-B channels activate slowly over hundreds of milliseconds, with openings to the fully open state that are ∼6-fold longer than those for Slack-A channels. In numerical simulations, neurones in which outward currents are dominated by a Slack-A-like conductance adapt very rapidly to repeated or maintained stimulation over a wide range of stimulus strengths. In contrast, Slack-B currents promote rhythmic firing during maintained stimulation, and allow adaptation rate to vary with stimulus strength. Using an antibody that recognizes all amino-termini isoforms of Slack, Slack immunoreactivity is present at locations that have no Slack-B-specific staining, including olfactory bulb glomeruli and the dendrites of hippocampal neurones, suggesting that Slack channels with alternate amino-termini such as Slack-A channels are present at these locations. Our data suggest that alternative promoters of the *Slack* gene differentially modulate the properties of neurones.

(Resubmitted 5 August 2008; accepted after revision 7 September 2008; first published online 11 September 2008)
Corresponding author L. K. Kaczmarek: Department of Pharmacology, Yale University School of Medicine, 333 Cedar Street, New Haven, CT 06520, USA. Email: leonard.kaczmarek@yale.edu

The diverse firing patterns of neurones can, in large part, be attributed to the specific types of K^+ channels expressed in these cells (Levitan & Kaczmarek, 2002). A subset of K^+ channels are regulated by intracellular ligands such as Na^+ and Ca^{2+} ions, and, as a result, can integrate multiple cellular signals and respond to patterns of neuronal firing over the relatively slow time course of stimulus-induced changes in the levels of these ions. K^+ channels sensitive to changes in intracellular Na^+ have been termed K_{Na} channels. These channels have been proposed to protect cardiomyocytes from elevated intracellular Na^+ during hypoxia as loss of oxygen diminishes the activity of plasma membrane Na^+,K^+-ATPases (Kameyama *et al.* 1984; Dryer, 1994). K_{Na} channels also contribute to the resting potential and excitability of neurones. K_{Na} channels contribute to the slow afterhyperpolarization following repetitive firing in a variety of neurones (Kameyama *et al.* 1984; Foehring *et al.* 1989; Schwindt *et al.* 1989; Kubota & Saito, 1991; Kim & McCormick, 1998; Sandler *et al.* 1998; Sanchez-Vives *et al.* 2000; Franceschetti *et al.* 2003; Descalzo *et al.* 2005). In high-frequency firing auditory neurones of the medial nucleus of the trapezoid body (MNTB), K_{Na} channels have been shown to regulate the accuracy of the timing of

 DOI: 10.1113/jphysiol.2008.160861

action potentials to varying rates of stimulation (Yang *et al.* 2007).

The activation of K_{Na} channels following stimulation has been reported to persist over a very wide range of time scales (from ~100 ms to several minutes; Bhattacharjee & Kaczmarek, 2005). In addition to the very different time courses over which K_{Na} channels have been reported to function in native cells, their reported properties at the single channel level are somewhat diverse. Reported EC_{50} values for Na^+ range from 7 to 80 mM and the unitary conductances vary from 100 to 200 pS with multiple subconductance states (Dryer, 1994), suggesting that the K_{Na} channels may be quite diverse at the molecular level.

One class of K_{Na} channels are encoded by the *Slack* gene (also called Slo2.2) (Joiner *et al.* 1998; Bhattacharjee *et al.* 2003; Yuan *et al.* 2003). These channels were first characterized for their large single channel conductance, which is similar but slightly lower than that of Slo1 Ca^{2+}-activated K^+ channels (for reviews see Bhattacharjee & Kaczmarek, 2005; Salkoff *et al.* 2006). However, Slack shares only 7% sequence homology with Slo1 and is activated by Na^+ instead of Ca^{2+}. Slack channels contain six putative membrane-spanning domains, a P-region between transmembrane domains 5 and 6, and an extensive carboxyl-terminus region. Unlike Slo1, the amino-terminus of Slack is predicted to be cytosolic.

In response to depolarization, Slack whole-cell currents typically activate slowly, and steady states are achieved only after several hundred milliseconds (Joiner *et al.* 1998; Bhattacharjee *et al.* 2003). Slack channels have a large single channel unitary conductance and multiple subconductance states (Bhattacharjee *et al.* 2003; Yuan *et al.* 2003). Native K_{Na} channels in MNTB neurones and other cell types generally have unitary conductances similar to those of Slack in stably transfected cells (Bhattacharjee *et al.* 2003; Yang *et al.* 2006, 2007). Slack K_{Na} channel subunits are highly expressed in the rat central nervous system according to immunohistochemical studies (Bhattacharjee *et al.* 2002).

In this study, we report the existence of multiple *Slack* transcripts that arise by alternative RNA splicing and that differ in the sequence of the predicted cytoplasmic amino-termini. Two of these give rise to alternative isoforms of *Slack* termed *Slack-A*. The kinetics of activation and single channel properties of Slack-A channels are quite distinct from the previously described Slack channels, which we now term Slack-B. The expression of Slack-A channels is regulated by a different promoter from that controlling the expression of other isoforms. Immunohistochemical studies indicate that amino-terminal Slack variants differ in their cellular localization in the nervous system. Numerical simulations indicate that the different kinetic properties of Slack-A and Slack-B channels are likely to contribute to quite different patterns of response to repetitive or sustained stimulation. Multiple Slack isoforms offer explanations for the varied contribution of native K_{Na} channels to the firing pattern of a neurone.

Methods

Molecular biology

Initial cloning of the *Slack-A* gene was performed using the Basic Local Alignment Sequence Tool algorithm (Altschul *et al.* 1990) using the amino acid sequence of the amino-terminus of *SLICK* (Bhattacharjee *et al.* 2003) against the human genome in GenBank. In addition to the match on chromosome 1, where *SLICK* is localized, a strong match was also identified on chromosome 9q34.3 approximately 14 kb upstream of the *SLACK* gene. Orthologues of the same putative exon were found in the rat and mouse genomes in GenBank. Primers were designed for amplifying cDNA using PCR to the 5′ UTR region of this putative exon in the rat genome and the known 3′ UTR of rat *Slack* (*rSlack*) (Joiner *et al.* 1998). Using a rat cDNA library as template and Pfu Turbo (Stratagene, La Jolla, CA, USA), a specific product was amplified, subcloned using the TA cloning kit (Invitrogen, Carlsbad, CA, USA), and sequenced (W.M. Keck Biotechnology Resource Center, Yale University). The *rSlack-A* cDNA was subcloned into the *Not*I and *Apa*I sites of the expression plasmid pTRACER (Invitrogen), for expression in Chinese hamster ovary (CHO) cells. The *rSlack-A* sequence has been submitted to GenBank (AY884213).

A detailed analysis of the 5′ region of the Slack gene was performed using a 5′ RNA ligase-mediated rapid amplification of cDNA ends (RLM-RACE) technique (GeneRacer Kit, Invitrogen). All experimental protocols involving animals were approved by the Yale University Animal Use and Care Committee. Briefly, 8-week-old C57BL/6 male mice were anaesthesized by open drop anaesthesia with methoxyflurane (Medical Developments International, Springdale, Australia) followed by decapitation. Brain and liver tissue was rapidly isolated and homogenized in Trizol reagent (Invitrogen), followed by precipitation of total RNA with isopropyl alcohol. Total RNA was cleaned using Qiagen RNeasy minispin columns (Valencia, CA, USA). For selection of full length mature capped mRNA, the total RNA was incubated with calf intestinal phosphatase and RNA was precipitated. The cap was removed from full-length mRNA with tobacco acid pyrophosphatase and remaining mRNA was precipitated. The 5′ phosphate of the isolated mRNAs was ligated to an RNA oligonucleotide. A cDNA library was generated using random hexamers. Next, PCR was performed on the cDNA library with a 5′ primer targeted to the RNA oligonucleotide (CGACTGGAGCACGAGGACACTGA) and a 3′ gene specific primer (GSP) designed to target exon 3 of *mSlack*

(TTGAGCCGCTCTTTGAAGGTGTTC). As a positive control, a 3′ primer to the *actin* gene (GACCTGGCCGTCAGGCAGCTCG) was also used in combination with the 5′ primer to the RNA oligonucleotide.

In separate experiments, total RNA was isolated and treated with DNase I (Qiagen) to remove contaminating genomic DNA before RT-PCR was performed using primers designed to target the regions of the 5′ untranslated regions (UTR) of the Slack transcripts (*mSlack-A*: GCGCGCGACCGGCGAGGGCG; *mSlack-B*: TAGCGCTCCCGCAGGATGGC; *mSlack-M*: ATAGTCAGTCCTAGCGAGGCACTG and the same 3′ GSP from the RLM-RACE experiments mentioned above).

To clone the *rSlack-A* and *rSlack-B* promoters, primers were designed for amplifying genomic DNA 2 kb upstream of the start of either *Slack-A* amino-terminus (forward primer CACTGACATAGCCATCTCAAAGGAGAGCG; reverse primer ATTGTGTGGCTGGCAGCGTCCAGGAG) or *Slack-B* amino-terminus (forward primer CCCATCTTCTTCCTTCCCTGAGCCGTC and reverse primer ATCCTGCGGGAGCGCTTGGCGC). Using PCR-ready rat genomic DNA (Biochain, Hayward CA, USA) and Pfu Turbo, 2 kb products were amplified and subcloned using the TA cloning kit (Invitrogen), and sequenced. Products were then subcloned into pGL3 luciferase reporter vector (Promega, Madison WI, USA). To create the *rSlick* channel containing the amino-terminus of *Slack-B*, a silent mutation was created in the transmembrane domain 1 region of both channels to generate a *Xho*1 site in each channel. The cDNAs for both channels were then subcloned into pcDNA 3.1 where the *Xho*1 site was deleted in the poly linker after the ligation. The amino-terminus was switched and verified by sequencing.

Promoter analysis

PC-12 cells were grown in DMEM medium supplemented with 10% heat-inactivated horse serum, 5% fetal bovine serum, penicillin and streptomycin (Gibco). Cells were plated in 24-well culture dishes at 90% confluence. Using LipofectAMINE 2000 (Invitrogen), cells were co-transfected with the firefly pGL3 luciferase constructs and a CMV-Renilla luciferase vector to control for transfection efficiency. Cells were harvested 48 h after transfection, lysed and then firefly and Renilla luciferase activities were measured using the Dual-luciferase Reporter Assay System (Promega) per manufacturer's guidelines. Experiments were performed in triplicate and repeated three times. Data were analysed using a one-way ANOVA and a Newman–Keuls *post hoc* test.

Real-time PCR

Real-time PCR was performed on the StepOne Real-time PCR system (Applied Biosystems; Foster City, CA, USA) using TaqMan gene expression assays (Applied Biosystems) specific to three Slack amino isoforms (Assay Mm00558471_m1: spanning exon 1b and exon 3; Assay Mm01330657_m1 spanning exon 1b and exon 2; custom assay to Slack-Ax2 spanning exon 1a and exon 3). RNA was isolated from 8-week-old male C57BL/6 mice as described earlier from the olfactory bulb, brainstem, cortex, hippocampus, whole brain and liver ($n = 3$). Random primers were used to generate cDNA from the same amount of RNA from each tissue, using the high-capacity cDNA reverse transcription kit (Applied Biosystems). All real-time PCR quantification was performed with a non-template control and the endogenous control GAPDH. The gene expression levels were interpolated from standard curves for relative expression and normalized to GAPDH in the same tissue. The normalized GAPDH values were divided by the whole brain value for each isoform assay to determine the fold expression change. In a separate analysis, the normalized GAPDH values were calibrated to the expression of a TaqMan assay targeting an internal exon–exon junction (Assay Mm01330663_m1: spanning exon 3 and exon 4) common to all amino-termini Slack isoforms from each tissue. Differences in the expression levels of Slack amino-termini isoforms were analysed using the unpaired Student's *t* test with $P < 0.05$.

Immunohistochemistry

A polyclonal pan-Slack antibody was designed against the carboxyl-terminus region of rSlack using the peptide sequence GCDVMNRVNLGYLQDEMNH. Generation of this rabbit polyclonal anti-pan-Slack IgG was carried out by Biosynthesis Inc. (Lewisville, TX, USA). The antibody against the amino-terminus of Slack-B was used in previous studies (Bhattacharjee *et al.* 2002). Antibodies were affinity-purified and DAB immunohistochemistry was performed as previously described (Bhattacharjee *et al.* 2002), using 2-month-old male C57BL6 mice brain slices (30–40 μm thick). For experiments utilizing immunofluorescence, 2-month-old C57BL6 mice were anaesthetized with sodium pentobarbital (60 mg kg^{-1}, I.P.) and perfused through the left ventricle with a PBS solution (100 mM Na_2HPO_4–NaH_2PO_4, pH 7.4, and 150 mM NaCl) containing 0.5% $NaNO_2$ and 1000 U heparin, followed by a phosphate buffer (PB) solution (100 mM Na_2HPO_4–NaH_2PO_4, pH 7.2) containing 4% paraformaldehyde. Brains were removed, post-fixed in 4% paraformaldehyde for 2 h at 4°C, rinsed twice with PB, and placed either in 30% sucrose at 4°C for 24 h or immediately sliced sagittally on a vibratome (20 μm thick). Brains not sectioned were embedded in O.C.T. compound (Tissue-Tek, Torrance, CA, USA), rapidly frozen in acetone containing dry ice, and stored at −80°C

until cryostat sectioning. Vibratome-cut sagittal (20 μm) slices were collected in multi-well plates containing PBS. Slices were then post-fixed in 4% paraformaldehyde for 5 min, followed by two washes with 1× PBS (for 5–10 min on an orbital shaker). Slices were permeabilized with a 1× PBS solution containing 1% bovine serum albumin (BSA), 5% normal donkey serum, 0.2% glycine, 0.2% lysine and 0.2% Triton X-100 (blocking solution) for 1 h at room temperature or 4°C overnight. Next, the slices were rinsed twice with PBS containing 1% BSA alone. Free-floating sections (20 μm thick) were processed for double labelling with chicken anti-Slack B (800 ng ml^{-1}) and rabbit anti-pan-Slack (1 : 500). After 48–72 h of incubation at 4°C in primary antibody, sections were washed three times for 10 min. Slack-B and pan-Slack antibodies were localized with Cy2 donkey anti-chicken and Cy3 donkey anti-rabbit (Jackson Immuno Research, West Grove, PA, USA) secondary antibodies, respectively, for 60 min at room temperature. Sections were mounted on glass slides, air dried, and coverslipped with 2.5% DL-2-amino-5-phosphonovaleric acid–1,4-diazabicyclo(2.2.2)octane (PVA-DABCO). Control sections were processed through similar immunohistological procedures, except the primary or secondary antibodies were omitted. In all cases, the omission of primary or secondary antibodies resulted in the lack of specific labelling.

Image acquisition and analysis

DAB images were taken with a Zeiss Axiophot microscope fitted with AxioCam HRc using AxioVision software. The scale bars on the DAB images are 100 μm. Fluorescent sections were examined with a Zeiss laser scanning microscope (LSM 510 META) using Zeiss image acquisition and analysis software. Images were acquired in the multi-track mode allowing for several tracks to be defined in one configuration for the scan procedure. Multi-track mode does not allow fluorescence to bleed into other channels. Images were acquired using a C-Apochromat 25× objective (with water correction) for brain slices and the optical thickness of the slices was constant for both tracks. Cy2 has excitation/emission of 496 nm/519 nm, and Cy3 has excitation/emission of 550 nm/570 nm. Double-immunofluorescence images were displayed as dual-colour merged images and the scale bar represents 50 or 100 μm on fluorescent images from MNTB brain slices.

Electrophysiology

For whole-cell recordings, chinese hamster ovary (CHO) cells were maintained and transiently transfected with vector constructs as previously described (Bhattacharjee *et al.* 2003). Electrodes had a resistance of 2–3 MΩ for whole-cell recordings and the bath solution contained (mM): 140 NaCl, 1 $CaCl_2$, 5 KCl, 29 glucose and 25 Hepes (pH 7.4). The pipette solution contained (mM): 130 KCl, 5 EGTA and 10 Hepes (pH 7.3). Under these conditions, there is sufficient sodium that enters through a presumed leak channel or other entry pathways to allow measurements of macroscopic currents (Joiner *et al.* 1998; Bhattacharjee *et al.* 2003).

For single channel recordings, Slack-B and Slack-A cDNAs were expressed in *Xenopus* oocytes. Slack-B was subcloned into the pOX vector (Yuan *et al.* 2003) and Slack-A was subcloned into the pMAX vector, a modified version of a dual vector pRAT (Bockenhauer *et al.* 2001). mRNA was prepared from appropriately linearized plasmid DNA with the mMessage mMachine T3 or T7 RNA kit from Ambion (Austin, TX, USA). The mRNA was purified using QIAquick PCR purification columns from Qiagen (Valencia, CA, USA). For single channel experiments, each oocyte was injected with 50 nl of the mRNA solution. Injected oocytes were kept at 18°C in a standard MND96 solution containing (mM): 88 NaCl, 1 KCl, 2 $MgCl_2$, 1.8 $CaCl_2$, 5 glucose, 5 Hepes and 5 pyruvate, pH 7.6. For patch clamp recordings of single channel currents, *Xenopus* oocytes were manually devitellinized in a hypertonic solution consisting of (mM): 220 sodium aspartate, 10 KCl, 2 $MgCl_2$, 10 Hepes and then placed in the MND96 solution with no added Ca^{2+} for recovery. Internal patch pipette solutions (IPS) used for recording consisted of (mM): 140 KCl, 5 NaCl, 5 EGTA, 1 $CaCl_2$, 1 $MgCl_2$, 5 Hepes and pH was adjusted to 7.5 with KOH. Cell-attached and excised inside-out patch recordings were done in symmetrical 140 mM KCl solutions with 5 mM Na^+. Single channel currents in *Xenopus* oocytes were recorded using an Axopatch 1D amplifier (Axon Instruments, Inc.). Currents were filtered at 1 kHz and data were acquired at 10 kHz. Data were analysed using pCLAMP 9 (Molecular Devices) and Origin 6.0 (Microcal Software, Northampton, MA, USA).

Numerical simulations

Simulations were carried out using a model similar to that previously described to simulate firing patterns of rapidly firing neurones and of the effects of K_{Na} currents on firing patterns (Liu & Kaczmarek, 1998; Wang *et al.* 1998; Richardson & Kaczmarek, 2000; Macica *et al.* 2003; Bhattacharjee *et al.* 2005; Song *et al.* 2005; Yang *et al.* 2007). Responses were simulated by integration of the equation $C\,dV/dt = I_{ext(t)} - I_{Na} - I_{Kv} - I_{KNa} - I_L$, where I_{Na} represents Na^+ current, I_{Kv} represents a high-threshold voltage-dependent K^+ current that contributes to action

potential repolarization, I_{KNa} represents a Na^+-activated K^+ current with kinetic properties matching those of either Slack-A or Slack-B, I_L is the leak current and stimuli $I_{ext(t)}$ were presented either as a single step current (0.01–0.11 nA, 400 ms) or as a train of brief repetitive current pulses (0.25 ms, 0.6 nA) of 100–200 Hz. Equations and parameters for I_{Kv} and I_L were identical to those in Macica *et al.* (2003), and are based on fits to currents in neurones of auditory brainstem, with parameters for I_{Kv} matching those for the Kv3.1 potassium channel and with $g_{Kv} = 0.15\ \mu S$. The capacitance C of the model cell was 0.01 nF.

I_{Na} and I_L were given by the equations $I_{Na} = g_{Na} m^3 h(V - E_{Na})$ and $I_L = g_L(V - 63)$, respectively. Kinetic parameters for the evolution of the variables m and h were $g_{Na} = 0.4\ \mu S$, $k_{\alpha m} = 76.4\ ms^{-1}$, $\eta_{\alpha m} = 0.037\ mV^{-1}$, $k_{\beta m} = 6.93\ ms^{-1}$, $\eta_{\beta m} = -0.043\ mV^{-1}$, $k_{\alpha h} = 0.000135\ ms^{-1}$, $\eta_{\alpha h} = -0.1216\ mV^{-1}$, $k_{\beta h} = 2.0\ ms^{-1}$ and $\eta_{\beta h} = 0.0384\ mV^{-1}$. The leakage conductance g_L was $0.002\ \mu S$. In simulations, E_{Na}, the reversal potential for Na^+ ions, was either allowed to vary with changes in intracellular Na levels (Na_i) according to the equation $E_{Na} = 58 \log(120/[Na_i])$ or was fixed at +50 mV.

To simulate Slack-A currents, I_{KNa} was given by the equation $I_{KNa} = g_K n^2 s\,(V + 80)$, where the variable n describes voltage dependence and is governed by equations identical to those for the K_V channel with the parameters $g_{KNa} = 0.06\ \mu S$, $k_{\alpha n} = 1.38\ ms^{-1}$, $\eta_{\alpha n} = -0.0105\ mV^{-1}$, $k_{\beta n} = 0.5763\ ms^{-1}$ and $\eta_{\beta n} = -0.0355\ mV^{-1}$. For Slack-B currents, $I_{KNa} = g_K n s\,(V + 80)$ with $g_{KNa} = 0.05\ \mu S$, $k_{\alpha n} = 0.01\ ms^{-1}$, $\eta_{\alpha n} = -0.0044\ mV^{-1}$, $k_{\beta n} = 0.0164\ ms^{-1}$ and $\eta_{\beta n} = -0.0206\ mV^{-1}$. The variable s represents the proportion of Slack channels activated by $[Na^+]_i$ (see below).

Changes in $[Na^+]_i$ at the cytoplasmic face of the K_{Na} channels were modelled by the equation $d[Na^+]_i/dt = aI_{Na} + a' - b[Na^+]_i$, where the kinetic constants a and a′ represent Na^+ entry though voltage-dependent Na^+ channels and Na^+ leak, respectively, and b determines the rate of pumping of Na^+ out of the cell. In the model cell, $a = 0.025$, $a' = 0.025\ mM\ ms^{-1}$ and $b = 0.01\ ms^{-1}$. The variable s represents the proportion of Slack channels activated by $[Na^+]_i$, and evolves according to the equation $ds/dt = k_f\,[Na^+]_i\,(1 - s) - k_b s$, with $k_f = 4.48\ mM^{-1}\ ms^{-1}$ and $k_b = 200\ ms^{-1}$.

The abbreviations used are: K_{Na}, Na^+-activated K^+ channel; MNTB, medial nucleus of the trapezoid body; Slack, sequence like a Ca^{2+}-activated K^+ channel; Slick, sequence like an intermediate Ca^{2+}-activated K^+ channel; RCK, regulate the conductance of K^+; PKC, protein kinase C; RLM-RACE, 5′ RNA ligase-mediated rapid amplification of cDNA ends; CHO, Chinese hamster ovary; UTR, untranslated region.

Results

Novel Slack isoforms are controlled by different promoters and alternative splicing

The *SLACK* gene is encoded by over 30 exons (Fig. 1*A*). In humans, *SLACK* is localized to chromosome 9q34.3, in mice to chromosome 2, and in rats to chromosome 3. The exon that encodes the previously described amino-terminus of Slack (Joiner *et al.* 1998), which we shall now refer to as exon 1b, encodes an amino-terminal region that is highly conserved across species. There is a second gene *Slick* (Slo2.1) that also encodes K_{Na} channels (Bhattacharjee *et al.* 2003). Although Slack and Slick subunits share 74% sequence identity, the previously described amino-terminus of Slack shows no similarity to the amino-terminus of Slick (Bhattacharjee *et al.* 2003).

Using the TBlastN algorithm at the National Center for Biotechnology website and the amino acid sequence of the amino-terminus of Slick, we found a putative *Slack* exon, which we term exon 1a, approximately 14 kb upstream of the previously described amino-terminus of Slack (Fig. 1*A*). To determine if this represents an alternative isoform of *Slack*, PCR was performed on a rat cDNA library using primers designed against specific sequences of DNA in the putative 5′ UTR of this novel exon and the known 3′ UTR of *rSlack*. A full-length clone encoding a protein of 1203 amino acids was amplified by PCR and this alternative Slack isoform contained an amino-terminus nearly identical to that of rSlick. Because of the organization and location of this alternative exon 1a with respect to the full gene, we named this channel subunit Slack-A, and the original Slack subunit, although it was described earlier, will now be referred to as Slack-B (Fig. 1*B*). Slack-A and Slack-B differ only in their amino-termini sequences.

To further characterize the major 5′-capped mRNA transcripts of *Slack*, a detailed analysis of the mature *mSlack* transcripts from mouse brain was performed using 5′ RNA ligase-mediated rapid amplification of cDNA ends (RLM-RACE) (Fig. 1*B*). Mouse brain mRNA was isolated and modified using sequential phosphatase reactions to allow for selection of mature mRNA. A short RNA oligonucleotide was ligated to the 5′ end of all mature brain mRNAs. PCR reactions were performed using a 5′ primer to the RNA oligonucleotide and a 3′ primer designed to target exon 3 of *mSlack*.

The 5′ RLM-RACE experiments yielded four PCR products in the size range 221–302 bp (Fig. 1*C* and *D*). Sequencing of these PCR products revealed the four different 5′ mRNA transcripts summarized in Fig. 1*B*. The originally cloned *Slack* transcript (Slack-B) contains the 153 bp exon 1b followed by the 42 bp exon 2. The *Slack-A* transcript contains the novel first exon 1a, which is 13.8 kb upstream of exon 1b, followed by exon 2. Two additional

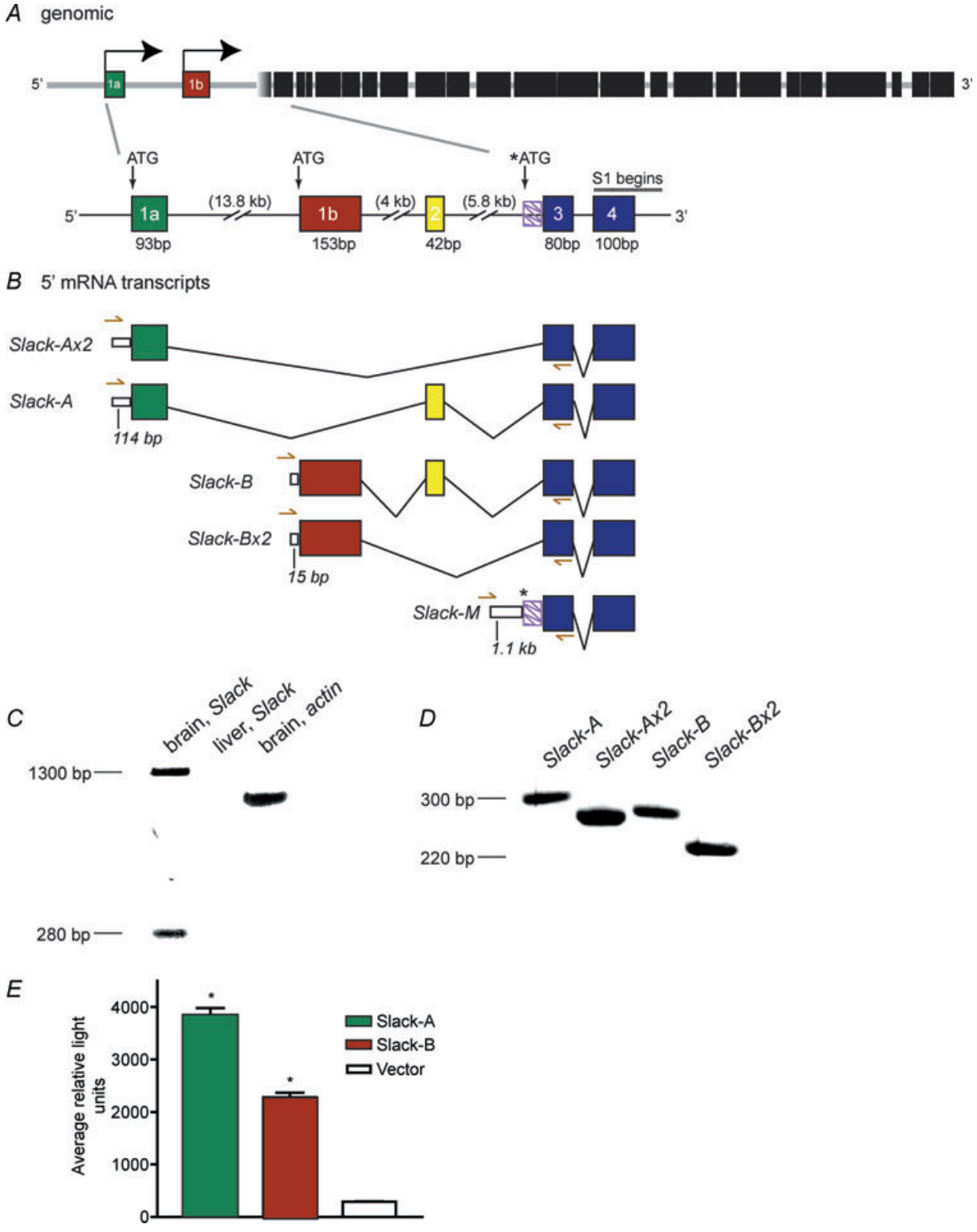

Figure 1. Alternative splicing of *Slack*

A, the *Slack* gene is located on chromosome 2 in mouse and contains over 30 exons. *B,* the major 5′-*Slack* isoforms produced in mouse brain were determined using 5′ RLM-RACE techniques. Different exons are depicted by boxes whereas the introns are shown by lines. The *mSlack-A* first exon 1a is ~13.8 kb upstream of the *mSlack-B* first exon 1b. The *mSlack-A* exon 1a is 40 bp smaller than the *mSlack-B* first exon. Exon 2 is also alternatively spliced and encodes a smaller 42 bp exon. A novel fifth RNA transcript, *mSlack-M*, beginning in the intron between exon 2 and 3, was detected using multiple techniques. All of the 5′ RNA transcripts described here involved changes to the

alternatively spliced transcripts of *Slack-A* and *Slack-B* were detected in which exon 2 was missing, and exons 1a or 1b were linked directly to exon 3 (*Slack Ax2* and *Slack Bx2*, Fig. 1*B* and *D*). The two *Slack-A* transcripts contain a 114 bp 5′ UTR between the start of transcription and the start of translation. In contrast, the two *Slack-B* transcripts contained only a 15 bp 5′ UTR after the start of transcription. None of the sequenced PCR products contained both exon 1a and exon 1b suggesting that these exons may be regulated by alternative promoters.

These experiments also detected a fifth putative *Slack* isoform, which contains a third novel first exon that is dissimilar to the first exon of *Slack-A* or *Slack-B*, and which we have termed *Slack-M*. In addition to the four PCR products described above, the 5′ RLM-RACE experiments yielded a single larger PCR product, 1330 bp in size (Fig. 1*C*). This *Slack-M* product was sequenced and found to contain a long 1.2 kb 5′ UTR sequence directly upstream of the beginning of exon 3 (Fig. 1*B*). As the first transmembrane domain S1 of *Slack* is encoded at the beginning of exon 4, all of the five mRNA transcripts described here reflect changes to the predicted cytoplasmic amino-terminus of the Slack channel.

The five different *Slack* transcripts (*Slack-A*, *Slack-Ax2*, *Slack-B*, *Slack-Bx2* and *Slack-M*) were also verified independently by isolating total RNA and degrading any contaminating genomic DNA in the sample with DNase I treatment followed by RT-PCR. Based on the sequencing results of RLM-RACE, primers targeting the 5′ UTR before exon 1a or exon 1b were used in combination with a reverse primer targeting the middle of exon 3 (primer locations marked in Fig. 1*B*). All five predicted products were detected. In contrast, no PCR products were detected in the negative control, which used the same primers on a cDNA library created from liver. This is consistent with previous northern analysis on the regional expression of *Slack* (Joiner *et al.* 1998), which found no *Slack* expression in liver (Fig. 1*C*). Positive control experiments were carried out using a 3′ primer targeted to the abundantly expressed actin mRNA in combination with the 5′ primer corresponding to the sequence ligated at the 5′ end of all mRNAs, and this produced the expected size PCR product in both brain and liver.

The existence of the two major classes of 5′-*Slack* transcripts (*Slack-A* and *Slack-B*) identified in the RLM-RACE experiments suggests that transcription of *Slack* is regulated by at least two different promoters. To test this hypothesis PC-12 cells were transfected with 2 kb of genomic DNA from the regions upstream of either exon 1a or exon 1b coupled to the gene for the luciferase reporter construct. Significant promoter activity for both *Slack-A* and *Slack-B* constructs was detected when compared to vector control (Fig. 1*E*). This finding demonstrates that the regions upstream of exon 1a or exon 1b are capable of acting as alternative sites for the recruitment of transcription machinery.

Slack-A, Slack-B and Slack-Bx2 mRNA are highly enriched in the olfactory bulb and brainstem

Previous *in situ* hybridization experiments using a probe against the 3′ UTR found widespread expression of *Slack* in many brain regions (Joiner *et al.* 1998) including regions such as the olfactory bulb and the auditory brainstem where K_{Na} channels have been characterized in depth (Yang *et al.* 2007). We used sequence specific real-time PCR to quantify the tissue distribution of amino-termini *Slack* isoforms in brain regions. Taqman gene expression assays were targeted to exon–exon junctions specific to the *Slack-Ax2*, *Slack-B* or *Slack-Bx2* isoforms (Fig. 2) to determine the relative mRNA expression of these transcripts. RNA was isolated from four different brain regions including brainstem, olfactory bulb, cortex

cytoplasmic amino-termini coding regions of the Slack protein. All products were sequenced and the experiments were repeated twice. A-3′ primer targeted to the middle of exon 3 was used in all experiments. *C*, the inverse image of the *mSlack-A* and *mSlack-B* RLM-RACE PCR products are shown as a band at 280 bp with the 3′ primer targeted for the middle of exon 3. A 1315 bp transcript is evident from the same preparation which contains a long sequence of 5′ UTR beginning between exon 2 and 3 of the *mSlack*. All products were sequenced and the experiment was repeated twice. As a negative control, RLM-RACE was also done on mRNA prepared from liver which does not have *Slack* expression (*C*, middle lane). A-3′ primer targeting the *β-actin* gene was used as a positive control using brain mRNA (*C*, last lane). *D*, additional analysis of the 5′ RACE products was performed by preparing brain mRNA and treating with DNase followed by RT-PCR with primers to the 5′ UTR of *mSlack-A* and *mSlack-B*, respectively. The same 3′ primer targeted to the middle of exon 3 was used. The inverse image of DNA electrophoresis bands is shown and demonstrated 4 transcripts verified by sequencing. The 280 bp band from the RACE experiments (in *C*) represented 4 transcripts (*mSlack-A, mSlack-Ax2, mSlack-B, mSlack-Bx2*) when run out on 2% agarose gel instead of a 1.2% agarose gel. *E*, *Slack* is under the control of alternative promoters. 2 kb of genomic DNA upstream encoding the different amino-termini of exon 1a for *rSlack-A* and exon 1b for *rSlack-B* were inserted into the pGL-3 vector, respectively. Promoter activity was assayed in PC-12 cells. Both the *Slack-A* and *Slack-B* promoter regions showed statistically significant ($P < 0.001$) luciferase activity compared to vector control. The *Slack-A* promoter was 2-fold higher in activity than *Slack-B* ($P < 0.001$). Experiments were performed in triplicate and repeated twice.

Table 1. Relative mRNA expression comparison within brain regions of *Slack* isoforms: *Slack-Ax2*, *Slack-B* and *Slack-Bx2*

	Slack-Ax2	*Slack-B*	*Slack-Bx2*	*Common exon*
Brainstem	3.44 ± 0.036	7.74 ± 0.798	13.01 ± 0.602	1.00 ± 0.011
Olfactory bulb	1.95 ± 0.022	4.60 ± 1.390	15.37 ± 0.997	1.00 ± 0.013
Cortex	1.29 ± 0.010	2.67 ± 0.055	4.05 ± 0.030	1.00 ± 0.007
Hippocampus	1.55 ± 0.014	4.79 ± 0.137	3.72 ± 0.037	1.00 ± 0.010
Liver	0.00 ± 0.000	0.00 ± 0.000	0.00 ± 0.000	1.00 ± 0.000
Whole brain	2.51 ± 0.343	2.07 ± 0.286	2.04 ± 0.279	1.00 ± 0.137

Slack-Bx2 mRNA was highly expressed in the brainstem and olfactory bulb compared to the *Slack-Ax2* and *Slack-B*. The relative expression for each *Slack* isoform was calibrated against the normalized value of a TaqMan assay detecting an exon–exon junction common to all amino-terminal *Slack* isoforms in each tissue. The results are expressed as mean ± S.E.M. ($n = 3$).

and hippocampus. All three isoforms were detected at significant levels in all brain regions tested. However, no *Slack* expression was detected in the RNA isolated from liver (Table 1) or in reactions where no template was included. The highest amount of *Slack-Ax2* expression was in the brainstem and olfactory bulb (Fig. 2). A similar pattern of tissue expression enrichment in the brainstem and olfactory bulb was seen for all the isoforms tested including *Slack-B* and *Slack-Bx2* (Fig. 2). There was less mRNA detected in the cortex and hippocampus for all three *Slack* isoforms.

We also compared mRNA expression for the amino-termini isoforms within the individual brain regions. The relative expression for each *Slack* isoform was calibrated against the normalized value of a TaqMan assay detecting an exon–exon junction common to all amino-termini *Slack* isoforms in each tissue. This assay detected mRNAs with exon 3 and exon 4 which was contained in all *Slack*

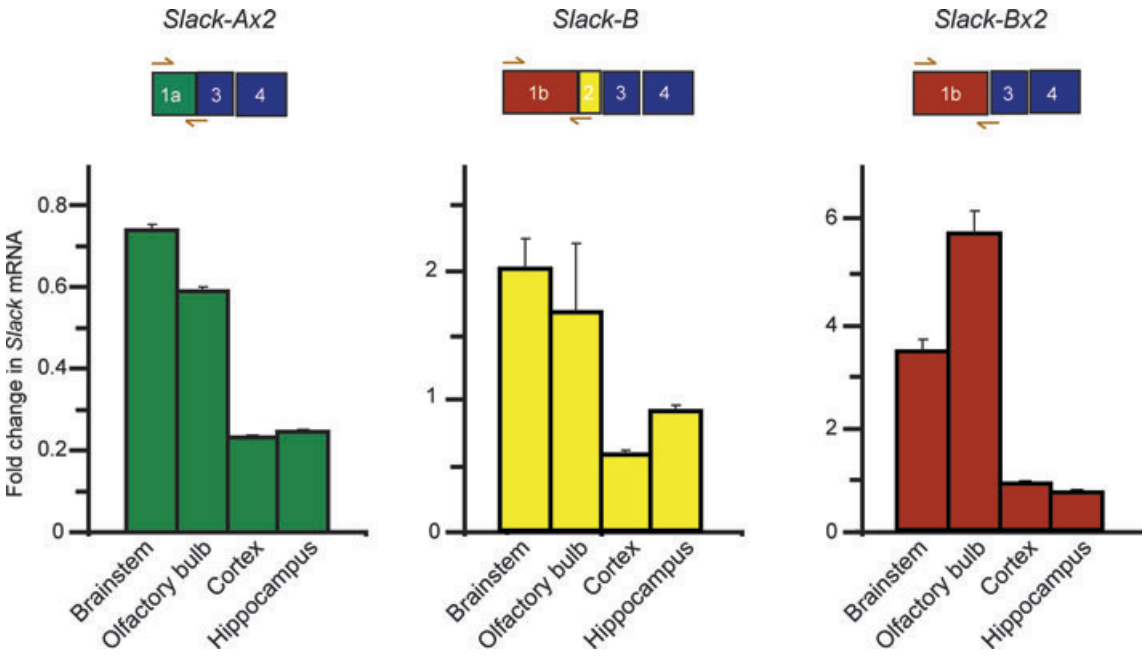

Figure 2. Real-time PCR quantification of Slack amino-termini isoforms in mouse brain
The relative expression levels of *Slack-Ax2*, *Slack-B* and *Slack-Bx2* isoforms were quantified across four different brain regions. Taqman assays were designed to specific exon–exon junctions at the 5′ end of the *Slack* gene to determine the relative abundance of *Slack* isoforms in the brain. There is a schematic diagram of the protein coding exons and the position of the primers used to identify a *Slack* isoform above each graph. *Slack-Ax2* mRNA levels were significantly enriched in the brainstem and olfactory bulb as compared to the cortex and hippocampus. In addition, *Slack-B* and *Slack-Bx2* mRNA expression was significantly higher in the brainstem and olfactory bulb samples. A significant signal was detected for all three isoforms tested in all four brain regions in comparison with no Slack detected in liver samples. The results are expressed as mean ± S.E.M. ($n = 3$).

isoforms described in this manuscript. The *Slack-Bx2* isoform was expressed 9.6-fold more than the *Slack-Ax2* isoform and 5.3-fold more than the *Slack-B* isoform in mRNA isolated from the brainstem (Table 1). *Slack-B* channel isoforms were higher in all of the brain regions tested; however, there were significant Slack-*Ax2* mRNAs detected in all brain regions.

Amino-termini of Slack-A subunits have a protein sequence similar to the Slick amino-terminus

Slack-B is highly conserved, with 95% amino acid identity across the mouse, rat and human genes (Bhattacharjee *et al.* 2003). The greatest deviation between Slack and Slick channels occurs in the amino-terminal regions of the proteins (Bhattacharjee *et al.* 2003). Slack-B subunits contain a first exon (1b encoding 52 amino acids) that is 1.6 times larger than the first exon of *Slick* or *Slack-A* (1a encoding 32 amino acids). Exon 1a encodes an amino acid sequence very similar to that of the first exon of *Slick* (Fig. 3*A*). There is 78.1% identity and 87.5% consensus between exon 1a of *Slack-A* and the first exon of *Slick*. In contrast, there is little similarity between *Slack* exons 1a and 1b (7.7% identity). All of the *Slack* transcripts described in these experiments have a common coding region that begins after exon 3. Thus, alternative promoters and splicing at the 5′ end of the *Slack* gene allows for the generation of channel isoforms with different cytosolic amino-terminal regions.

Slack isoforms have differential expression in the mouse brain

Immunohistochemistry in rat brain using an antibody targeted against the amino-terminal region of Slack-B subunits (Fig. 3*B*) found staining in many brain regions including the olfactory bulb and the MNTB in the auditory brainstem (Bhattacharjee *et al.* 2002). However, only limited Slack-B staining was found in certain brain regions such as the hippocampus, where Slack mRNA is also expressed. It is not practical to make an antibody against the amino-terminal end of Slack-A, because this would almost certainly cross-react with Slick. We have therefore generated a second anti-Slack antibody, targeted against

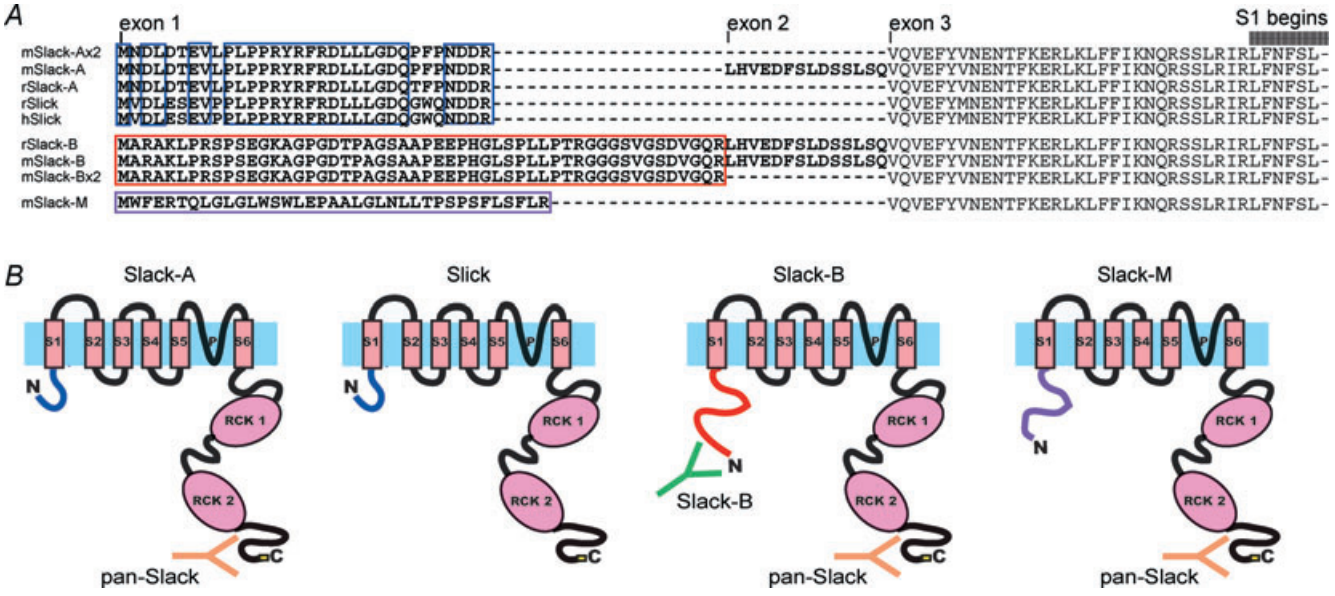

Figure 3. Amino acid sequence comparison for K_{Na} transcripts in mouse and rat
A. the protein encoded by exon 1a of *Slack-A* is highly homologous to that of *Slick* first exon as shown by the amino acid sequence alignment from isoforms in mice and rats. The protein abbreviations refer to: mSlack-Ax2: mouse *Slack-A* with exon 1a but without exon 2; mSlack-A: mouse *Slack-A* with exon 1a and exon 2; rSlack-A: rat *Slack* with exon 1a and no exon 2; rSlick: rat *Slick*; hSlick: human *Slick*; rSlack-B: rat *Slack-B* with exon 1b and exon 2; mSlack-B: mouse *Slack-B* with exon 1b and exon 2; mSlack-Bx2: mouse *Slack-B* with exon 1b and no exon 2; mSlack-M: novel predicted first exon with sequence before exon 3. All of the isoforms have similar sequence to exon 3 until the carboxyl terminal end of the protein. *B,* topological representations of two major isoforms of Slack. *Slack-A* contains an amino-terminus encoded by exon 1a and *Slack-B* contains an amino-terminus encoded by exon 1b. Both amino terminal ends are believed to be cytosolic. Two antibodies against Slack have been generated and the targets within the channel are indicated in the figure. The previously described antibody raised in chicken was targeted against the amino-terminal end of Slack-B and the pan-Slack antibody raised in rabbit is targeted against the carboxyl-terminal end common to all Slack amino isoforms.

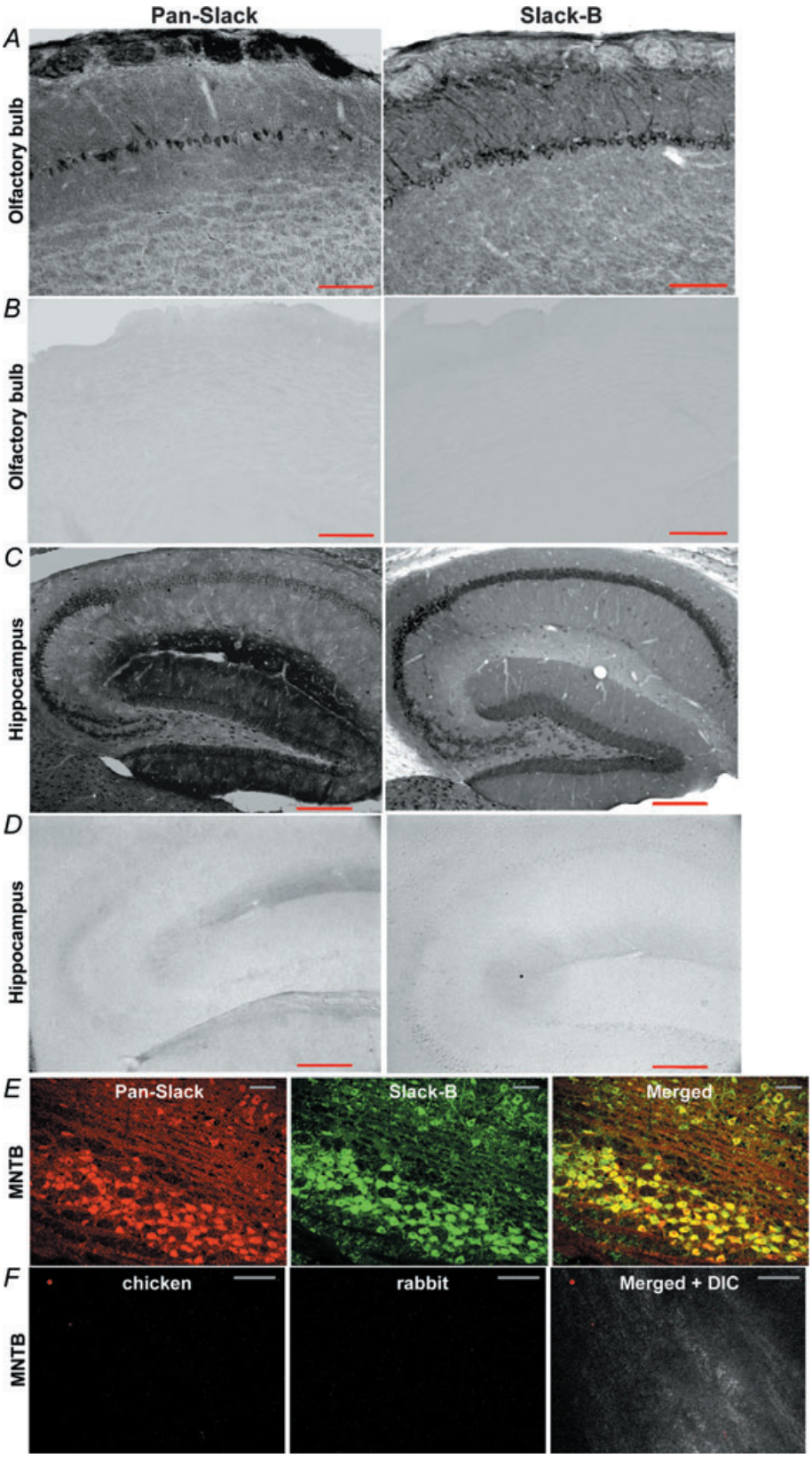

Figure 4. Immunohistochemical staining in mouse brain sections using two different Slack antibodies
C57Bl/6 mouse brain sections of the olfactory bulb (*A*) or the hippocampus (*C*) were stained with either rabbit anti-pan-Slack (left panel) or chicken anti-Slack-B (right panel) antibodies followed by DAB. The pan-Slack

the carboxyl-terminal region of Slack (Fig. 3*B*), which would be expected to recognize both Slack-A and Slack-B isoforms, but not to recognize Slick channels.

This pan-Slack antibody successfully labelled Slack-B-transfected CHO cells, but gave no staining with untransfected cells (data not shown). Strong immunoreactivity of neurones was found throughout the nervous system in sections of mouse brain stained with this antibody. We therefore compared the pattern of staining with this pan-Slack carboxyl-terminal antibody with that produced by staining with the Slack-B-specific amino-terminal antibodies in three brain regions: the olfactory bulb (Fig. 4*A*), hippocampus (Fig. 4*C*) and MNTB within the brainstem (Fig. 4*E*). When control sections were processed through the same immunohistological procedures except that the primary antibody was omitted, there was a complete lack of specific labelling (Fig. 4*B*, *D* and *F*).

In the olfactory bulb, the Slack-B immunoreactivity was strong in the mitral cell soma and dendrites as well as the tufted cells located superficially in the external plexiform layer below the glomeruli. While pan-Slack staining could be detected in these areas, including the mitral cells, the strongest pan-Slack immunoreactivity was located in the olfactory nerve layer and glomerular layer, which was devoid of Slack-B immunoreactivity (Fig. 4*A*).

In mouse hippocampus, staining for Slack-B was confined to the cell bodies of the CA2 and CA3 cells, with some additional staining in the CA1 cells (Fig. 4*C*). Slack-B immunoreactivity was also seen in the granule cells of the dentate gyrus but not in the dendrites of granule cells. While pan-Slack immunoreactivity was detected in the somata of these same cells, there was also very strong pan-Slack immunoreactivity in the dendrites of the granule cells and in the molecular layer of the dentate gyrus, regions that were negative for Slack-B.

In the MNTB, a region known to express high levels of Slack (Bhattacharjee *et al.* 2002), we performed co-immunofluorescence staining of sections with both pan-Slack and Slack-B (Fig. 4*E*). There was a strong co-localization of pan-Slack and Slack-B in the somata of the principal neurones of the MNTB.

Slack-A currents activate rapidly

In order to compare the electrophysiological properties of exon 1a-containing Slack-A channels with those of exon 1b-containing Slack-B channels, we transfected CHO cells with two different channel isoforms. Whole-cell currents in Slack-A-transfected cells (containing exon 1a and exon 2) activated very rapidly with step changes in voltage to test potentials positive to −50 mV (Fig. 5*A*). In their voltage dependence and kinetic behaviour, Slack-A currents were very similar to those recorded in Slick-transfected cells (Fig. 5*C*). In contrast, as has been reported previously (Joiner *et al.* 1998; Bhattacharjee *et al.* 2003), whole-cell currents of CHO cells transfected with Slack-B cDNA (containing exon 1b and exon 2), had an instantaneous component followed by a slower time-dependent increase in current that required several hundred milliseconds to attain steady state at positive potentials (Fig. 5*B*).

These findings suggest that the amino-termini of Slack and Slick channels are a primary determinant of the kinetic behaviour of these channels. To determine whether the amino-terminal region is the sole factor that regulates the rate of channel activation, we engineered a Slick channel that contains the amino-terminus of Slack-B, specifically with exon 1b and exon 2 of *Slack* attached to the rest of the *Slick* gene. CHO cells transfected with this construct, however, did not activate slowly in response to depolarization (Fig. 5*D*), but instead had a kinetic behaviour that more closely resembled wild-type Slick currents (Fig. 5*C*). This suggests that the amino-terminus of Slack-B coding for the region of exon 1b, cannot alone fully account for the slow activation properties of the Slack-B currents, which probably require interaction of the amino-terminus with a central region specific to the Slack channel.

Slack-A and Slack-B differ in their single channel behaviour

We also carried out a comparison of the behaviour of Slack-B and Slack-A channels at the single channel level using excised inside-out patches from occytes injected with cRNA for Slack-B or Slack-A. Patches were recorded under

antibody recognizes the carboxyl terminal end of Slack-A and Slack-B. In contrast the Slack-B antibody is targeted to the unique amino terminal end of Slack-B and does not recognize Slack-A. Neither of these antibodies recognizes Slick subunits. *E*, immunofluorescence of pan-Slack (far left panel, red) and Slack-B (middle panel, green) in sections from the MNTB. Co-localization in principal neurones immunoreactive to both antibodies is indicated in yellow (far right). Control sections with the primary antibody omitted showed no specific staining using the same immunohistochemical technique in olfactory bulb (*B*), hippocampus (*D*), and MNTB (*F*) with donkey anti-rabbit (left panels in *B,D and F*) and mouse anti-chicken (right panels in *B,D and F*). The far right panel in *F* is the merged fluorescent signal plus the differential interference contrast (DIC) to demonstrate the presence of the tissue in the images. The scale bar represents either 100 μm (in *A–E*) or 50 μm (in *F*).

conditions of symmetrical 140 mM KCl with 5 mM Na^+ on both sides of the membrane, and were maintained at potentials between +80 and −80 mV for tens of seconds. Consistent with earlier studies (Joiner *et al.* 1998; Bhattacharjee *et al.* 2003), Slack-B channels had large 'box-like' openings corresponding to a unitary conductance of 177 ± 8 pS ($n = 7$, Fig. 6*A* and *D*). As has also been previously reported, subconductance states could readily be detected in recordings of Slack-B channels (Fig. 6*A* and *C*).

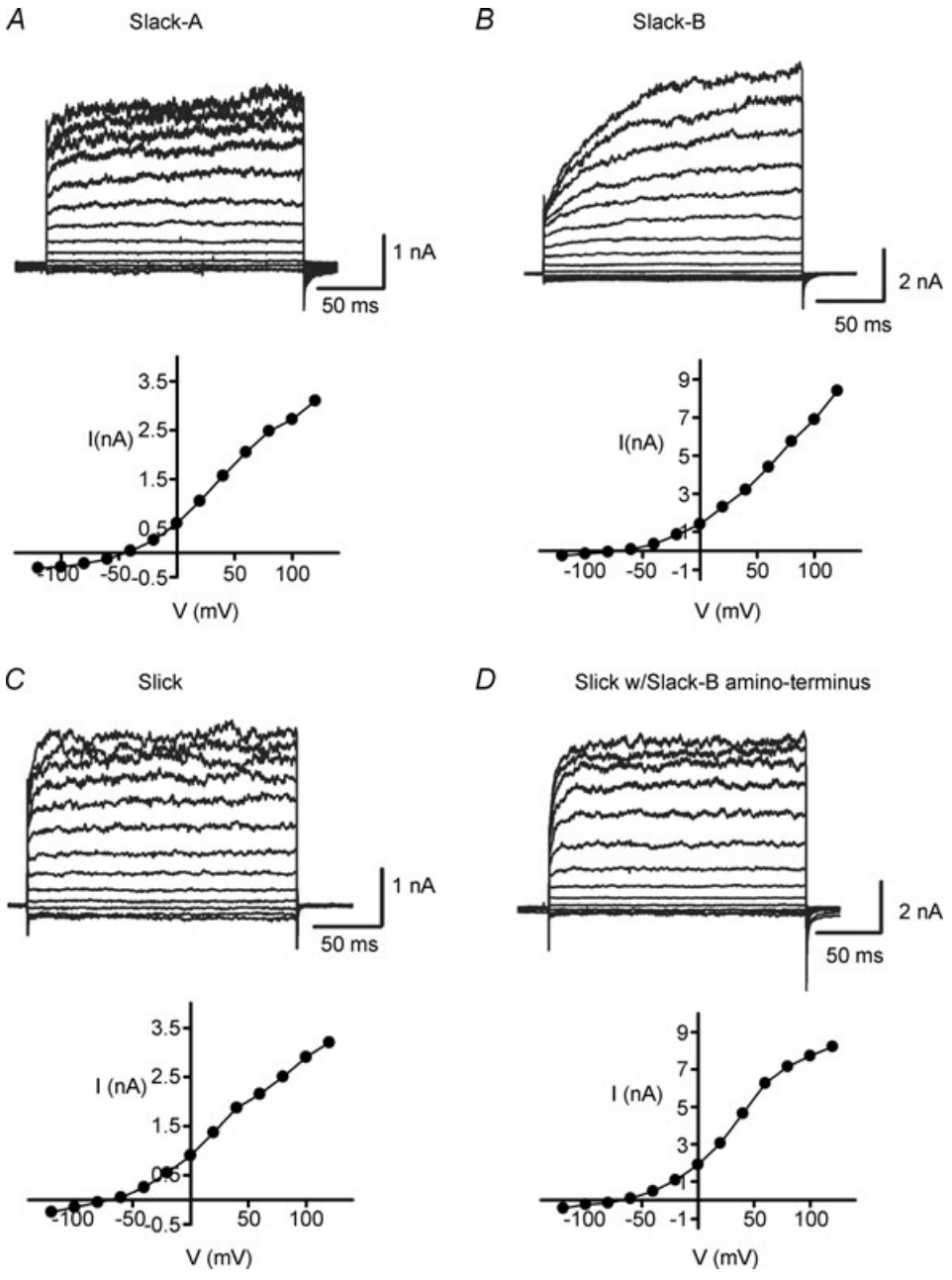

Figure 5. Slack-A currents activate rapidly
Whole-cell recordings of CHO cells transfected with *Slack-A* containing exon 1a (*A*), *Slack-B* containing exon 1b (*B*), *Slick* (*C*), and a *Slick* construct containing exon 1b amino-terminus of *Slack-B* with the rest of *Slick* (*D*) are shown. Slack-A and Slick currents activate very rapidly with step changes in voltage. This contrasts with Slack-B currents, which exhibit an instantaneous component followed by a slow time-dependent increase in current, particularly at higher voltages. A mutated Slick channel containing the amino-terminus of Slack-B did not, however, show similar slow gating properties (*D*).

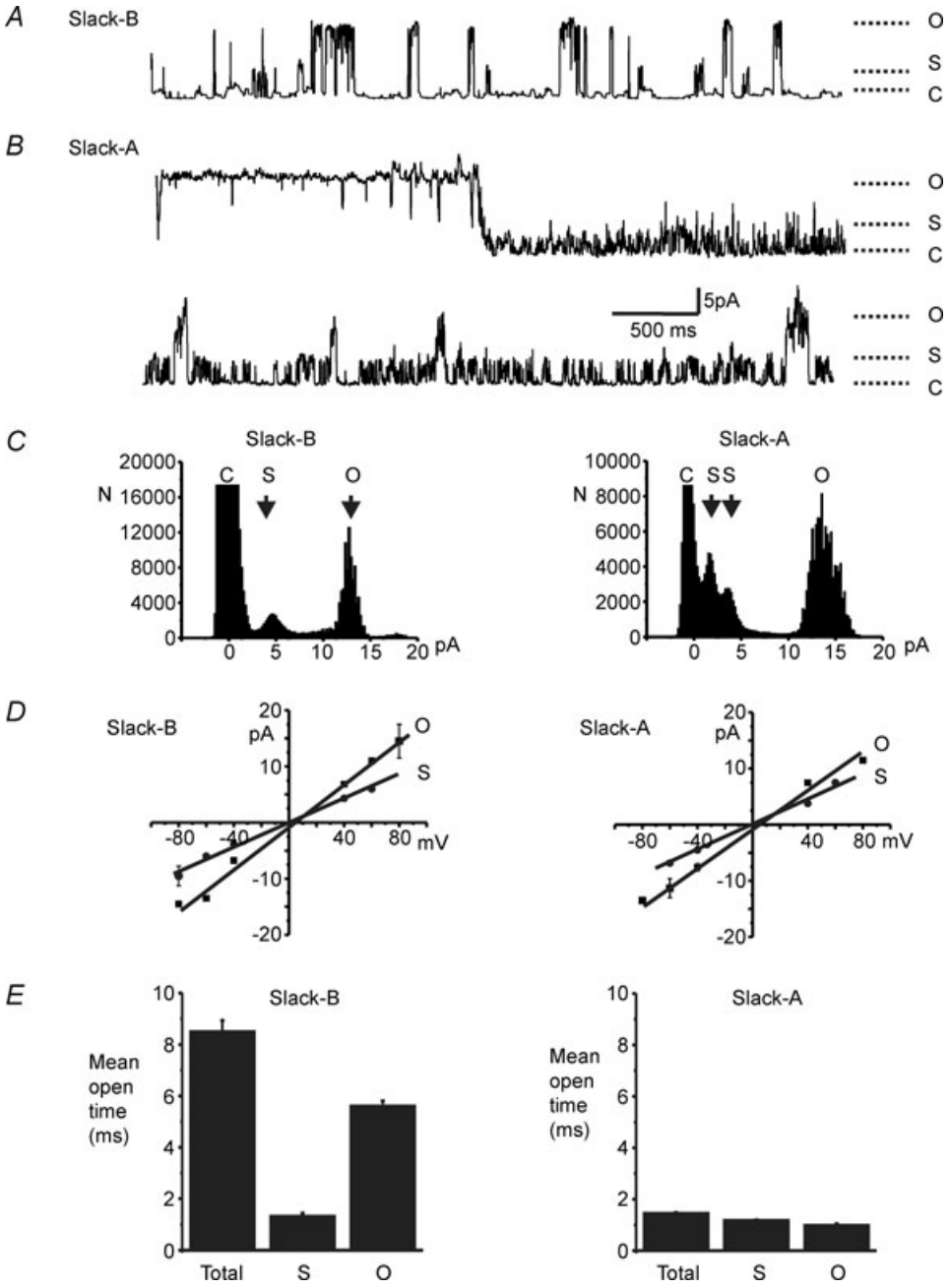

Figure 6. Comparison of the unitary activity of Slack-B and Slack-A channels
A, representative trace of Slack-B channel activity recorded in an excised inside out patch held at −80 mV with symmetrical solutions containing 140 mM KCl with 5 mM Na^+ on both sides of the membrane. Channel activity was recorded after keeping the patch at −80 mV for over 10 s following a step from to 0 mV to −80 mV. Closed (C), fully open (O) and major subconductance (S) levels are indicated. *B*, representative traces of Slack-B channel activity recorded in an excised inside out patch under the same conditions as in *A*. Upper trace shows activity recorded within the first 10 s following a step from 0 mV to −80 mV. During this time, a prolonged opening to the fully open state changes to a pattern of brief openings to subconductance states. The lower trace shows a recording from the same patch after the potential had been held at −80 mV for over 10 s. Brief openings to both fully open and subconductance states can be observed. *C*, all points amplitude histograms for patches expressing Slack-B or Slack-A channels. Closed (C), fully open (O) and major subconductance levels (S) are indicated. *D*, mean open channel *I–V* relations for Slack-B and Slack-A channels. Data are shown both for the fully open state and for the largest subconductance state. Amplitudes were determined from amplitude histograms such as those in *B*, and represent mean values from 4 and 5 patches for Slack-B and Slack-A channels, respectively. *E*, total mean open times and individual mean open times for the fully open and subconductance states for Slack-B and Slack-A channels after being held at −80 mV for at least 10 s ($N = 4,5$ for Slack-B, Slack-A channel-containing patches, respectively).

Like Slack-B, Slack-A channels had a large unitary conductance (180 ± 8 pS) that was statistically indistinguishable from that of Slack-B (Fig. 6*C*). Prolonged openings to this fully open state were most evident after stepping the patch potential to a negative value (+80 mV in Fig. 6*B*). After maintaining the patch at such a potential for 10 s, activity changed to a pattern in which brief transient openings to the fully open state were interspersed with repeated opening to subconductance states. These subconductance states were generally more prominent in Slack-A channels than in Slack-B channels (Fig. 6*C*). Two or more prominent subconductance levels could clearly be detected in five of Slack-A-expressing patches whereas only a single subconductance state could be resolved in 3 of 4 Slack-B-expressing patch, and in the fourth patch, two subconductance states were only resolved at a potential of −80 or +80 mV.

The kinetic behaviour of Slack-B and Slack-A channels was quite distinct. Taking into account subconductance states as well as openings to the full open state, the mean open time of Slack-B channels was over six times longer than that of Slack-A channels (measured at a patch potential of +80 mV, Fig. 6*E*). This increase in mean open time could in large part be attributed to significantly longer openings to the fully open state for Slack-B channels. Such openings were ∼6-fold longer than those for Slack-A (Fig. 6*E*). In contrast, the openings to the largest subconductance level were not significantly different in duration in Slack-B and Slack-A channels (Fig. 6*E*).

Slack-A and Slack-B differentially affect rhythmic firing and adaptation in model neurones

In different neuronal types, activation of K_{Na} currents has been proposed either to act very rapidly, influencing membrane properties after only one or two action potentials or to develop only during periods of firing lasting tens of seconds or more (Dryer, 1994; Bhattacharjee *et al.* 2005). To evaluate how the expression of different isoforms of the Slack channel may influence the timing of neuronal adaptation we carried out numerical simulations of a model neurone expressing equivalent levels of either Slack-A- or Slack-B-like currents. For these simulations we modified a neuronal model of auditory brainstem neurones that has been previously used to investigate the general effects of K_{Na} currents on neuronal firing (Yang *et al.* 2007). The single-compartment model incorporated a voltage-dependent Na^+ current, a 'high-threshold' delayed rectifier voltage-dependent K^+ current, a leakage conductance and a Na^+-activated K^+ current with kinetic parameters matching those of either Slack-A or Slack-B (Fig. 7*A*). Levels of conductance were adjusted such that, in the absence of the Na^+-activated K^+ current, the cell was not spontaneously active at rest, but fired continually high-frequency simulation with brief current pulses (Fig. 7*B*). The voltage dependence of both Slack isoforms is such that, following an elevation of internal Na^+, these channels open near the resting potential. Thus, as expected, introduction of either Slack-B- or Slack-A-like currents into the model neurone increased the current threshold for action potential generation and slowed the rate of firing during prolonged repetitive simulation (Fig. 7*B*, see also Fig. 9). The slower rate of activation of Slack-B channels, however, permitted the generation of repeated rhythmic bursts of action potential stimulation, over a wide range of stimulus parameters. In contrast, model neurones expressing the same level of conductance of Slack-A-like current typically fired only for a brief period at the onset of the stimulus train (Fig. 7*B*).

Another difference between simulations incorporating Slack-B or Slack-A currents was that the rate of adaptation at the onset of the stimulus train was always slower for Slack-B-containing neurones. This is demonstrated in Fig. 8*A*, which shows the response to a much shorter stimulus train for neurones with the same model and stimulus parameters as in Fig. 7*B*. A clear analysis of the role of Slack channels in adaptation of firing rate in such models is complicated by the fact that, as intracellular Na^+ accumulates during stimulation, the reversal potential for Na^+ ions (E_{Na}) is reduced. This leads to a progressive decrease in action potential height and, in response to intense maintained stimulation, produces an adaptation of firing rate independent of K^+ channel activity. To circumvent this problem, we carried out additional simulations in which the Na^+ current was rendered insensitive to intracellular Na^+ levels. Computationally this was achieved simply by fixing E_{Na} at +50 mV, and can be considered to correspond to a mechanism that increases sodium channel conductance to compensate for changes in E_{Na}. Such a simplified model allows one selectively to evaluate the way that the kinetic properties of Slack isoforms contribute to adaptation. Both of the phenomena of bursting during maintained repetitive stimulation and the slower rate of adaptation in Slack-B-containing model neurones are retained in this simplified model (Fig. 8*B*). In addition, the slower rate of adaptation in Slack-B-containing neurones can be clearly seen in the simulation of the response of Slack-B- or Slack-A-containing cells to a maintained depolarizing current step (Fig. 8*C*).

To further evaluate the effects of the kinetic differences between Slack-B and Slack-A on firing patterns, we compared the responses of the simplified model neurones to depolarizing current pulses of increasing amplitude. The control cells, lacking Na^+-activated K^+ currents, were not spontaneously active at rest, but fired continually to depolarizing current pulses (Fig. 9). The addition of equal levels of either Slack-B or Slack-A conductances raised the

threshold for action potential generations and prevented firing in response to very weak depolarizing currents. As the stimulus strength was increased in Slack-B-containing neurones, the duration for which firing of action potentials could be evoked progressively increased, and, at the highest stimulus strengths, firing persisted through the period of depolarization, but an adaptation of firing rate could be observed during the pulse (Fig. 9). In contrast, in the

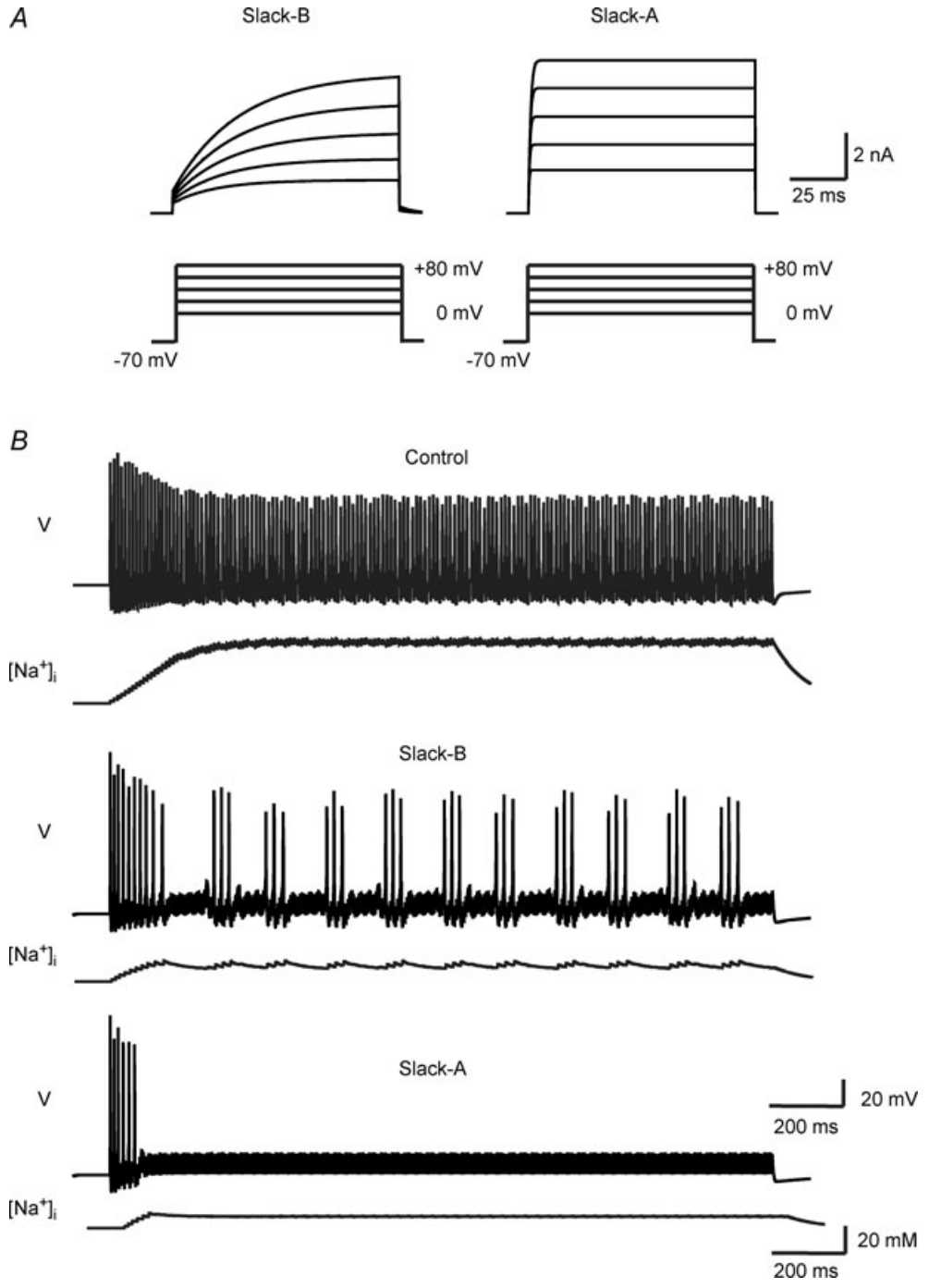

Figure 7. Numerical simulations of the effects of Slack-B and Slack-A currents on firing of a model neuron

A, Slack-B and Slack-A simulated currents evoked by test depolarizations from a holding potential of −70 mV to test potentials between 0 and +80 mV. *B*, response of the model neurone with no Na^+-activated K^+ current or with the same conductance of Slack-B or Slack-A current to a 1.8 s train of depolarizing current pulses (0.6 nA, 0.25 ms) applied at 200 Hz. Upper traces in each case show membrane potential (V) and lower traces shown levels of intracellular Na^+.

Slack-A-containing cells, rapid adaptation occurred at all stimulus strengths (Fig. 9). At no stimulus strength could action potential firing be extended beyond the very onset of the stimulus pulse, and with very high stimulus currents, the early action potentials were further reduced by inactivation of Na^+ current (not shown).

Discussion

In this study, we have identified an alternative isoform of *Slack*, Slack-A, which contains a different amino-terminus from the previously described isoform, Slack-B. Other isoforms of *Slack* identified include variants with and without a 14 amino acid exon coding for a short region of the cytoplasmic amino terminus domain. Two different experimental techniques also confirmed the existence of mRNA encoding a further *Slack* isoform, *Slack-M*, which contains a third novel first exon with no similarity to the first exon of either *Slack-A* or *Slack-B*. We have shown that the genomic DNA upstream of the exons encoding the amino-terminus of *Slack-A* and *Slack-B* both have significant promoter activity. Although genes under the control of multiple promoters are common for other types of proteins (Landry *et al.* 2003), the use of alternative promoters appears to be unusual for ion channels. The Kv3.4 channel (Vullhorst *et al.* 2001) and the IP_3 receptor (Gower *et al.* 2001) have been shown to be under the control of multiple promoters. As is the case for Kv3.4, the alternative amino-termini of Slack influence the kinetic properties of the currents.

Previous *in situ* hybridization studies (Joiner *et al.* 1998) using the 3′ UTR region of *Slack* as a probe, found widespread expression of *Slack* in rat brain. We used sequence-specific quantitative real-time PCR to discriminate between three amino-termini isoforms which were all found to be highly expressed in the olfactory bulb and brainstem regions. Lower levels of *Slack-Ax2*, *Slack-B* and *Slack-Bx2* mRNA were detected in the cortex and hippocampus regions. Immunohistochemical studies in rat found a more restricted pattern of expression of Slack-B protein (Bhattacharjee *et al.* 2002). Our present experiments are consistent with this finding, as we

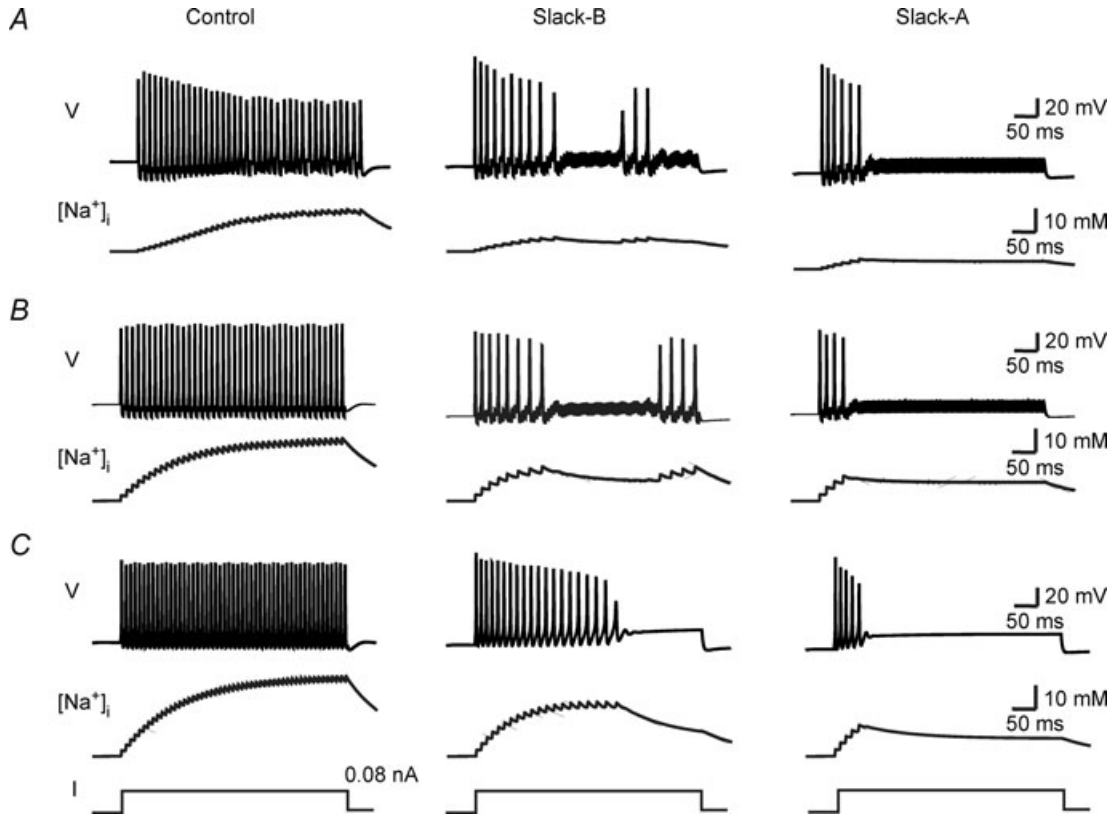

Figure 8. Numerical simulations of the effects of Slack-B and Slack-A currents on adaptation of firing rate

A, response of control and Slack-B- and Slack-A-containing cells to a 400 ms train of depolarizing current pulses (0.6 nA, 0.25 ms) applied at 200 Hz. *B*, response of control and Slack-B and Slack-A containing cells to the same stimuli as in *A* in a simplified model in which voltage-dependent Na^+ current was not reduced by elevations in internal Na^+. *C*, response of the simplified neurones in *B* to a single 400 ms depolarizing current pulse (0.08 nA). Upper traces in each case show membrane potential (V) and lower traces shown levels of intracellular Na^+.

demonstrated differences in the immunohistochemical localization of antibodies detecting Slack-B alone with that of a novel pan-Slack antibody, which would be expected to detect all amino-terminal Slack variant proteins. In particular, pan-Slack distribution in olfactory bulb and hippocampus was more widespread than that of Slack-B itself. Currently it is not possible to determine whether the Slack immunoreactivity in olfactory glomeruli or

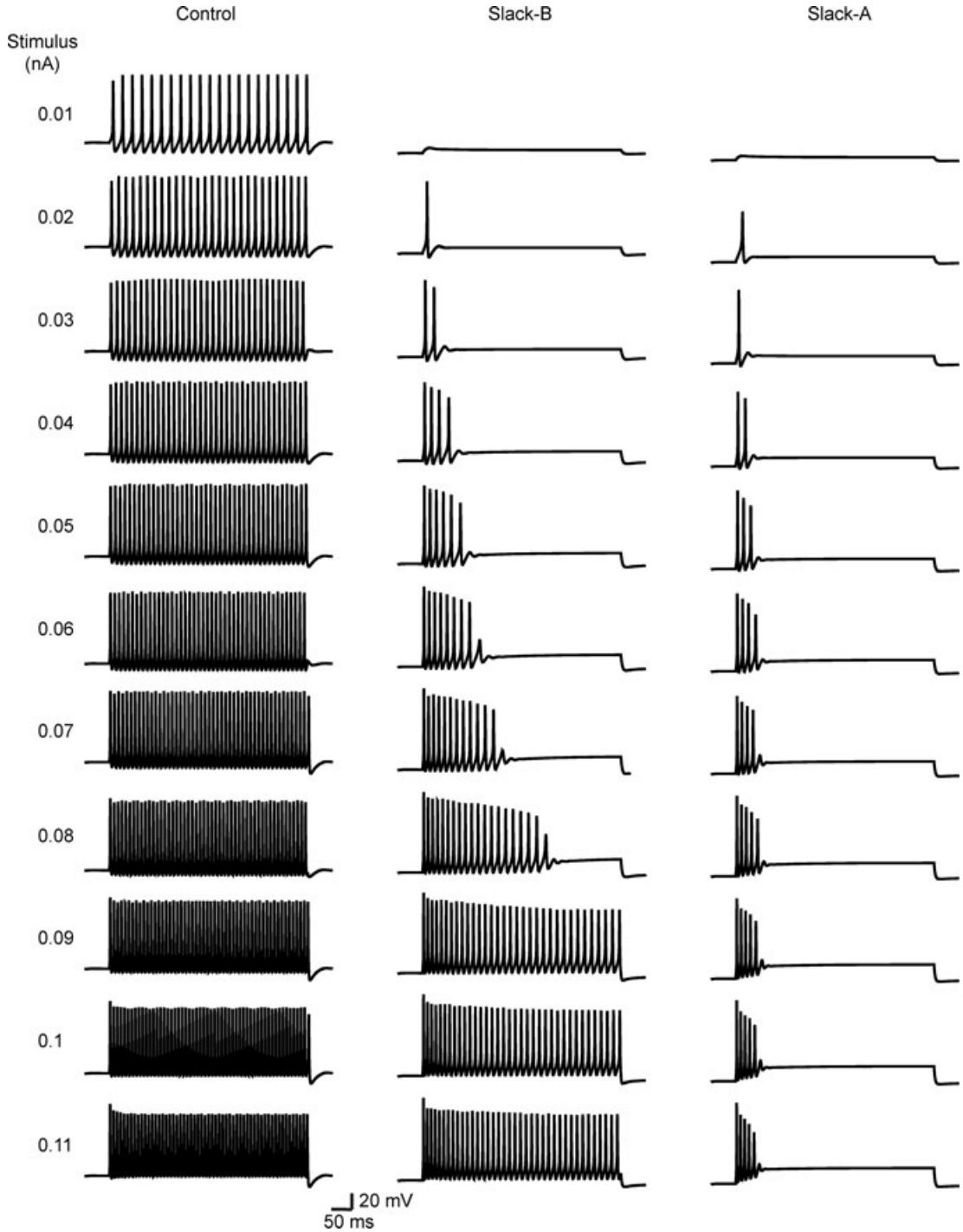

Figure 9. Numerical simulations of the response of control and Slack-B- and Slack-A-containing model neurones to depolarizing currents of increasing amplitude
As the stimulus strength was increased in Slack-B-containing neurones, the duration for which firing of action potentials could be evoked progressively increased. In contrast, in the Slack-A-containing cells, rapid adaptation occurred at all stimulus strengths. A simplified model in which voltage-dependent Na^+ current was not reduced by elevations in internal Na^+ was used in these simulations.

hippocampal dendrites reflects the presence of Slack-A or Slack-M proteins. In addition, we cannot eliminate the possibility that additional splice variants of the *Slack* gene arise from splicing at the 3′ end.

The amino-terminus of Slack-A channels is similar to that of Slick channels. While Slick subunits, like Slack, are widely distributed in the nervous system (Bhattacharjee *et al.* 2005), one functional difference between Slack and Slick subunits is that Slick channels are potently suppressed by ATP binding to a site on the Slick carboxyl-terminus. Thus, the role of Slick subunits under physiological levels of ATP is not yet known. Like Slick channels (Bhattacharjee *et al.* 2003), Slack-A whole-cell currents activate very rapidly in response to depolarization with no slow time-dependent component of activation. Our findings have shown that the kinetic properties of Slack-A and Slack-B channels, at both the macroscopic and single channel levels, are quite distinct, and that the amino-terminus of Slack-B is required for the slow activation of this isoform following depolarization. It appears, however, that another component within the Slack channel is also required for slow gating in Slack-B. In particular, a Slick construct containing the amino-terminus of Slack-B did not exhibit slow activation.

Recent studies have shown that K_{Na} channels contribute to burst firing and to adaptation in a variety of different neurones including cortical neurones (Schwindt *et al.* 1989; Franceschetti *et al.* 2003), thalamic neurones (Kim & McCormick, 1998) and trigeminal neurones (Sandler *et al.* 1998). Specifically, K_{Na} facilitates slow afterhyperpolarizations (Dryer, 1994; Franceschetti *et al.* 2003) and can regulate the duration of depolarizing after-potentials (Liu & Stan Leung, 2004). Our numerical simulation of the kinetic properties of Slack-A and Slack-B isoforms indicate that the predominance of one or other of these isoforms is likely to shape the specific pattern of response to repetitive stimulation. In particular, Slack-B channels are likely to promote bursting and a graded pattern of adaptation, whereas Slack-A channels are more likely to produce a strong and fixed pattern of rapid adaptation. Our simulations used model cells in which these Slack isoforms were the dominant potassium currents active near the resting potential. Naturally, in real neurones, the influence of these channels will be integrated with those of other channels that shape firing patterns. Specific determination of how the expression of the rapidly activating Slack-A or slowly activating Slack-B isoforms contributes differentially to these patterns of firing will require genetic or other manipulations specifically to alter the activity of these K_{Na} channels in native neurones.

References

Altschul SF, Gish W, Miller W, Myers EW & Lipman DJ (1990). Basic local alignment search tool. *J Mol Biol* **215**, 403–410.

Bhattacharjee A, Gan L & Kaczmarek LK (2002). Localization of the Slack potassium channel in the rat central nervous system. *J Comp Neurol* **454**, 241–254.

Bhattacharjee A, Joiner WJ, Wu M, Yang Y, Sigworth FJ & Kaczmarek LK (2003). Slick (Slo2.1), a rapidly-gating sodium-activated potassium channel inhibited by ATP. *J Neurosci* **23**, 11681–11691.

Bhattacharjee A & Kaczmarek LK (2005). For K^+ channels, Na^+ is the new Ca^{2+}. *Trends Neurosci* **28**, 422–428.

Bhattacharjee A, Von Hehn CA, Mei X & Kaczmarek LK (2005). Localization of the Na^+-activated K^+ channel Slick in the rat central nervous system. *J Comp Neurol* **484**, 80–92.

Bockenhauer D, Zilberberg N & Goldstein SA (2001). KCNK2: reversible conversion of a hippocampal potassium leak into a voltage-dependent channel. *Nat Neurosci* **4**, 486–491.

Descalzo VF, Nowak LG, Brumberg JC, McCormick DA & Sanchez-Vives MV (2005). Slow adaptation in fast-spiking neurons of visual cortex. *J Neurophysiol* **93**, 1111–1118.

Dryer SE (1994). Na^+-activated K^+ channels: a new family of large-conductance ion channels. *Trends Neurosci* **17**, 155–160.

Foehring RC, Schwindt PC & Crill WE (1989). Norepinephrine selectively reduces slow Ca^{2+}- and Na^+-mediated K^+ currents in cat neocortical neurons. *J Neurophysiol* **61**, 245–256.

Franceschetti S, Lavazza T, Curia G, Aracri P, Panzica F, Sancini G, Avanzini G & Magistretti J (2003). Na^+-activated K^+ current contributes to postexcitatory hyperpolarization in neocortical intrinsically bursting neurons. *J Neurophysiol* **89**, 2101–2111.

Gower NJ, Temple GR, Schein JE, Marra M, Walker DS & Baylis HA (2001). Dissection of the promoter region of the inositol 1,4,5-trisphosphate receptor gene, itr-1, in *C. elegans*: a molecular basis for cell-specific expression of IP3R isoforms. *J Mol Biol* **306**, 145–157.

Joiner WJ, Tang MD, Wang LY, Dworetzky SI, Boissard CG, Gan L, Gribkoff VK & Kaczmarek LK (1998). Formation of intermediate-conductance calcium-activated potassium channels by interaction of Slack and Slo subunits. *Nat Neurosci* **1**, 462–469.

Kameyama M, Kakei M, Sato R, Shibasaki T, Matsuda H & Irisawa H (1984). Intracellular Na^+ activates a K^+ channel in mammalian cardiac cells. *Nature* **309**, 354–356.

Kim U & McCormick DA (1998). Functional and ionic properties of a slow afterhyperpolarization in ferret perigeniculate neurons *in vitro*. *J Neurophysiol* **80**, 1222–1235.

Kubota M & Saito N (1991). Sodium- and calcium-dependent conductances of neurones in the zebra finch hyperstriatum ventrale pars caudale *in vitro*. *J Physiol* **440**, 131–142.

Landry JR, Mager DL & Wilhelm BT (2003). Complex controls: the role of alternative promoters in mammalian genomes. *Trends Genet* **19**, 640–648.

Levitan IB & Kaczmarek LK (2002). *The Neuron: Cell and Molecular Biology*. Oxford University Press, Oxford, New York.

Liu SQ & Kaczmarek LK (1998). Depolarization selectively increases the expression of the Kv3.1 potassium channel in developing inferior colliculus neurons. *J Neurosci* **18**, 8758–8769.

Liu X & Stan Leung L (2004). Sodium-activated potassium conductance participates in the depolarizing afterpotential following a single action potential in rat hippocampal CA1 pyramidal cells. *Brain Res* **1023**, 185–192.

Macica CM, Von Hehn CA, Wang LY, Ho CS, Yokoyama S, Joho RH & Kaczmarek LK (2003). Modulation of the kv3.1b potassium channel isoform adjusts the fidelity of the firing pattern of auditory neurons. *J Neurosci* **23**, 1133–1141.

Richardson FC & Kaczmarek LK (2000). Modification of delayed rectifier potassium currents by the Kv9.1 potassium channel subunit. *Hear Res* **147**, 21–30.

Salkoff L, Butler A, Ferreira G, Santi C & Wei A (2006). High-conductance potassium channels of the SLO family. *Nat Rev Neurosci* **7**, 921–931.

Sanchez-Vives MV, Nowak LG & McCormick DA (2000). Cellular mechanisms of long-lasting adaptation in visual cortical neurons *in vitro*. *J Neurosci* **20**, 4286–4299.

Sandler VM, Puil E & Schwarz DW (1998). Intrinsic response properties of bursting neurons in the nucleus principalis trigemini of the gerbil. *Neuroscience* **83**, 891–904.

Schwindt PC, Spain WJ & Crill WE (1989). Long-lasting reduction of excitability by a sodium-dependent potassium current in cat neocortical neurons. *J Neurophysiol* **61**, 233–244.

Song P, Yang Y, Barnes-Davies M, Bhattacharjee A, Hamann M, Forsythe ID, Oliver DL & Kaczmarek LK (2005). Acoustic environment determines phosphorylation state of the Kv3.1 potassium channel in auditory neurons. *Nat Neurosci* **8**, 1335–1342.

Vullhorst D, Jockusch H & Bartsch JW (2001). The genomic basis of K_V, 3.4 potassium channel mRNA diversity in mice. *Gene* **264**, 29–35.

Wang LY, Gan L, Forsythe ID & Kaczmarek LK (1998). Contribution of the Kv3.1 potassium channel to high-frequency firing in mouse auditory neurones. *J Physiol* **509**, 183–194.

Yang B, Desai R & Kaczmarek LK (2007). Slack and Slick K_{Na} channels regulate the accuracy of timing of auditory neurons. *J Neurosci* **27**, 2617–2627.

Yang B, Gribkoff VK, Pan J, Damagnez V, Dworetzky SI, Boissard CG, Bhattacharjee A, Yan Y, Sigworth FJ & Kaczmarek LK (2006). Pharmacological activation and inhibition of Slack (Slo2.2) channels. *Neuropharmacology* **51**, 896–906.

Yuan A, Santi CM, Wei A, Wang ZW, Pollak K, Nonet M, Kaczmarek L, Crowder CM & Salkoff L (2003). The sodium-activated potassium channel is encoded by a member of the Slo gene family. *Neuron* **37**, 765–773.

Acknowledgements

This research was supported by grants from the National Institutes of Health (NS42202, DC01919) to L.K.K. and (NS61479) to M.R.B. We thank G. Rowe for technical assistance with the promoter studies and Applied Biosystems for use of real-time PCR machine.